

## RECENT DEVELOPMENTS IN CFD APPLIED TO VISCOUS AND NON-NEWTONIAN MIXING IN AGITATED VESSELS

Philippe A. TANGUY<sup>1</sup>, Mourad HENICHE<sup>1</sup>, Christian RIVERA<sup>1</sup>, Christophe DEVALS<sup>1</sup> and Katsuhide TAKENAKA<sup>2</sup>

<sup>1</sup> URPEI, Dept. of Chemical Engineering, Ecole Polytechnique, Montreal, CANADA

<sup>2</sup> SHI Mechanical & Equipment Inc., Saijo-City, Ehime, JAPAN

### ABSTRACT

Viscous and non-Newtonian fluid mechanics plays an important role in a large number of processes in the oil, mineral and chemical industries. In most situations of practical interest, the flow is in the laminar or in the transition regime due to the high viscosity of the products at hand. The use of CFD to tackle such problems is gaining in popularity, a good example of which is in mechanical mixing and reactor design. In CFD applied to mixing, the objectives are to select the best set of vessel configuration, impeller geometry, and operating conditions that provide an “optimal” performance for the wide range of rheological behaviors that may occur during processing. This presentation focuses on the development of advanced finite element CFD methods and their use for the design of viscous, Newtonian and non-Newtonian mixing processes in stirred tanks. It is illustrated with the performance of two modern mixing technologies namely, the multiple shaft mixer and the single-shaft multipurpose impeller mixer. It is shown that CFD can provide a lot of insight on the fluid mechanics in the reactor, and give access to mixer design parameters like the power consumption and the mixing time.

### NOMENCLATURE

$c$	concentration
$c_{ave}$	average concentration
$D$	diameter
$D_t$	diameter - turbine
$\mathbf{f}$	body force
$k$	consistency index
$n$	power law index
$nel$	number of elements
$N_a$	rotating speed – anchor
$N_t$	rotating speed – turbine
$Np$	power number
$p$	pressure
$P$	power
$Re$	Reynolds number
$\mathbf{r}$	residual
$\mathbf{v}$	velocity vector
$V$	volume
$t$	time
$\dot{\gamma}$	rate of deformation
$\rho$	density
$\eta$	viscosity function
$\mu$	dynamic viscosity
$\boldsymbol{\tau}$	stress tensor

### INTRODUCTION

Mixing is a generic operation in the process industries. The range of industrial applications is very wide, from flotation in the mining industry to the fabrication of personal care products like cosmetics and creams. The fluid rheology plays a major role in mixing as it governs the fluid mechanics in the process. This makes the design of a universal mixing system barely possible and, in practice, a good design will always be application-related. At least three factors can affect the effectiveness of a mixing system: the type of agitator, the flow regime and the fluid rheology.

The mixing of viscous and non-Newtonian fluids is particularly complex as the operation is usually carried out at low Reynolds number in the laminar or early transition regime, and the rheological properties may evolve considerably over the process and also vary significantly with the deformation rate in the vessel. To address these issues, several types of agitators have been introduced, mainly of the axial type to maximize the “top-to-bottom pumping”. These are the helical ribbon impellers with a single or double helix, the multiple shaft mixers typified by concentric coaxial mixers or planetary mixers, and the single-shaft multipurpose mixers, in particular the so-called class of wide impellers particularly popular in Japan.

In a coaxial mixer, the vessel is mounted with two concentric shafts supporting different types of agitators, rotating at different speeds and operated in either co-rotating or counter-rotating mode. They are gaining in popularity due to their flexibility and their relatively good efficiency over a wide range of Reynolds numbers. Scientific knowledge on their design is still poor and mainly based on empirical knowledge.

Wide impellers are made of a combination of large blades designed to guide the flow stream in the vessel. One example is the Maxblend (SHI Mechanical & Equipment) composed of a bottom paddle surmounted by a dispersing grid. This impeller installed with a small bottom clearance generally in a baffled vessel (an unbaffled vessel can be used at very low Reynolds number) generates a significant axial pumping even at low Reynolds numbers (Takahashi *et al.*, 2006), making it a good candidate for rheologically evolving media. The objective of this work is to show the capabilities of CFD to understand the fluid mechanics and describe the mixing characteristics in a coaxial mixer and a vessel mounted with the Maxblend impeller.

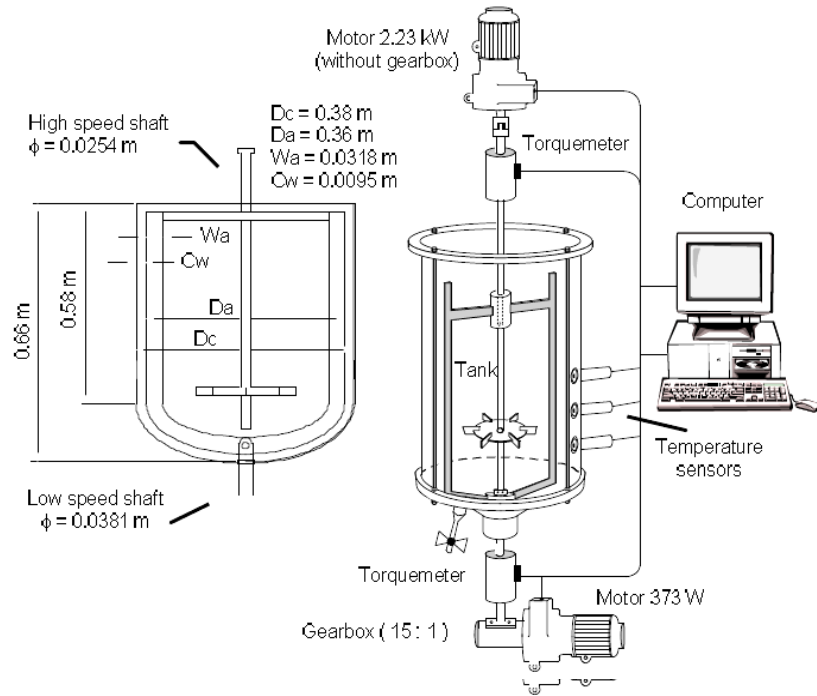


Figure 1: Schematic diagram of the coaxial mixer

## MIXER DESCRIPTION

The first mixer considered is a fully instrumented coaxial mixer of 46 L (Figure 1). It consists of two independently rotating coaxial shafts running respectively at high and low speed. The high-speed shaft drives a radial discharge Rushton turbine while the low speed shaft supports a wall scraping anchor arm. In the present work, 3 operating configurations are considered, namely co-rotating mode, counter-rotating mode and fixed anchor arm (equivalent to a two-baffle vessel).

The second mixer is based on the Maxblend technology (Figure 2). The rig is fully instrumented as for the coaxial setup except that the vessel volume is 200 L. The dimensions of the system are  $D_I = 450$  mm and  $H_I = 590$  mm, for the impeller and  $D_T = 600$  mm and  $H_T = 720$  mm for the tank. The Maxblend impeller can be operated with and without baffles. In this work, both configurations are investigated. For the baffled configurations, four identical baffles are employed. The dimensions of a baffle are the following: 7 mm thickness, 48 mm width and 570 mm height.



Figure 2: Maxblend impeller

The fluids used are aqueous solutions of corn syrup for Newtonian fluids and aqueous solutions of hydrocolloids for the non-Newtonian fluids. Their rheological properties have been determined with a Bohlin Viscometer 88-BV in a Couette-type configuration. The viscosity of the Newtonian fluids ranges between 1 and 10 Pa.s and the density is 1350 kg/m<sup>3</sup>. The non-Newtonian fluid rheology follows a power law model with the shear-thinning index ( $n$ ) and the consistency index ( $k$ ) varying according to the gum concentration (a few wt %). Their density is close to that of water (1000 kg/m<sup>3</sup>).

## NUMERICAL METHOD

When investigating the hydrodynamics performance of a mixer (power consumption and mixing time), it is traditional to model the fluid mechanics for a “homogeneous” single phase. In this case, the unsteady three-dimensional flow field is governed by the incompressible Navier-Stokes equations:

$$\rho \left( \frac{\partial \mathbf{v}}{\partial t} + \mathbf{v} \cdot \nabla \mathbf{v} \right) + \nabla p + \nabla \cdot \boldsymbol{\tau} = \mathbf{f}$$

$$\nabla \cdot \mathbf{v} = 0$$

The boundary conditions for the two mixing configurations are:

- No normal velocity at the (horizontal) fluid surface ( $v_z=0$ );
- No slip condition at the vessel wall and on the fixed structures (baffles) ( $\mathbf{v}=\mathbf{0}$ );
- Constant angular velocity on the impeller surfaces;
- In addition, for transient simulations the fluid is assumed initially at rest ( $\mathbf{v}=\mathbf{0}$ ,  $p=0$ ).

In this work, these equations are solved using a Galerkin finite element method with unstructured tetrahedral

meshes. To deal with the non-linearities associated with the non-Newtonian rheology, a classical augmented Lagrangian approach is adopted.

The pressure-velocity variables are treated in a coupled way with help of TFQMR (Freund, 1993) that belongs to the class of Krylov linear iterative solvers. In the case of the coaxial mixer and the Maxblend mixer with baffles, there is no simplifying Lagrangian frame of reference that can be used due to the absence of symmetry of revolution. In practice we keep to the conventional laboratory frame of reference (Eulerian viewpoint), and work with the fictitious domain method to reproduce the rotation of the agitators (Bertrand *et al.*, 1997).

The unstructured meshes of the two mixers have been generated with I-DEAS (EDS) software using block partitions. Due the complexity of the geometry, tetrahedral 9-node locally mass conserving elements  $P_1^+$ - $P_0$  that approximate the velocity with a super-linear polynomial and the pressure as a constant inside each element are employed. The final computational mesh requires approximately 290,000 elements producing a system of 2.1 M equations for the coaxial mixer and 110,000 elements yielding approximately 1.4 M equations for the Maxblend vessel. All the described numerical features are available in the commercial 3D finite element software POLY3D<sup>TM</sup> (Rheosoft, Inc.) developed in our group.

The computed hydrodynamics solutions have been considered converged when the maximum relative error for the Newton-Raphson scheme is smaller than 10%, that means:

$$100 \times \frac{\|\mathbf{v}^{(i+1)} - \mathbf{v}^{(i)}\|}{\|\mathbf{v}^{(i)}\|} \leq 10\%$$

In the above formula the superscript  $i$  stands for the Newton-Raphson fixed point iteration number. To avoid irregularities on the convergence caused by small velocities a sensibility of  $10^{-2}$  m/s has been employed. That means that velocity values smaller than the prescribed sensibility are not taken into account for this convergence criteria.

Furthermore, the solutions obtained by the Krylov ILU preconditioned TFQMR iterative linear solver have been considered converged when the ratio between the residual denoted  $\mathbf{r}^{(i)}$  (the superscript  $i$  stands for the iteration number) Euclidian norm and the first residual  $\mathbf{r}^{(0)}$  Euclidian norm is smaller than the prescribed tolerance  $\varepsilon$ . This can be expressed as

$$\frac{\|\mathbf{r}^{(i)}\|}{\|\mathbf{r}^{(0)}\|} \leq \varepsilon$$

In this study the value of  $\varepsilon$  was fixed to  $10^{-6}$ .

## POWER CONSUMPTION

In CFD applied to mixing, the power can be readily obtained through a standard macroscopic energy balance, namely:

$$P = \int_V \eta(\dot{\gamma}) \dot{\gamma} dV \text{ with } \dot{\gamma} = \dot{\gamma} : \dot{\gamma}$$

Experimentally, it is best determined by measuring directly the torque and the speed on each agitator. To establish the power master curve ( $Np$  vs.  $Re$  relationship), we have followed the approach of Foucault *et al.* (2004) in which the characteristic speed of the mixer is set in the co-rotating mode as  $N = N_t - N_a$ , and in the counter-rotating mode as  $N = N_t + N_a$ . With these definitions, the Reynolds number and the power number for each operating mode is defined as:

### Newtonian case

$$Re_{counter-rotation} = \frac{\rho(N_t + N_a)D_t^2}{\mu}$$

$$Re_{co-rotation} = \frac{\rho(N_t - N_a)D_t^2}{\mu}$$

### Non-Newtonian case

$$Re_{counter-rotation} = \frac{\rho(N_t + N_a)^{2-n} D_t^2}{k}$$

$$Re_{co-rotation} = \frac{\rho(N_t - N_a)^{2-n} D_t^2}{k}$$

Using these definitions, the power number is

$$Np_{counter-rotation} = \frac{P_{tot}}{\rho(N_t + N_a)^3 D_t^5}$$

$$Np_{co-rotation} = \frac{P_{tot}}{\rho(N_t - N_a)^3 D_t^5}$$

In the laminar regime, a common practice is to compare the power draw through a so-called power constant  $Kp$  which is nothing but the product of  $Np$  by  $Re$ . This constant is independent of the rotation speed and it is only a function of the geometry (impellers, vessel, and internals) and the rheology. It is useful to recall that the higher the  $Kp$  the higher the power consumption.

## MIXING TIMES

It is well known that in a batch reactor, the total energy to mix is obtained by multiplying the power by the mixing time. In mixing simulations, mixing times are typically obtained by tracking the evolution of the position of tracers launched at a given point in the vessel that would correspond to the injection point of tracers in a real vessel. The numerical tracers are massless, non-diffusing and non-interacting particles, and as such they do not represent a strict equivalent of a tracing dye or solid tracers particles in real experiments. They are, however, easy to compute and the experience shows that they provide a very good indication of the mixing mechanisms observed in physical experiments. In the present work, the injection point of the numerical tracers

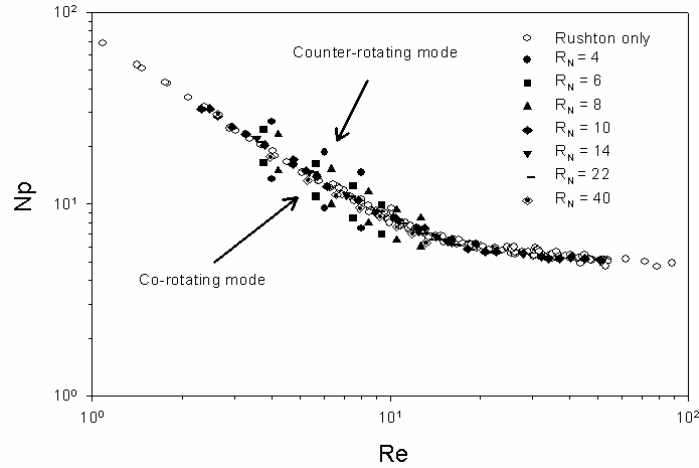


**Figure 3:** Coaxial experimental power consumption

is located at the top of the tank close to the shaft as in the real experiments. Mixing experiments are based on a color change from purple to yellow. To this end, a fast acid-base indicator reaction is used, consisting of a solution of 0.08% bromocresol purple as the indicator along with a basic solution of 10 N NaOH and an acidic solution of 10 N HCl.

## RESULTS

### Power Consumption

Let us first consider the coaxial mixer. Figure 3 shows the power curve for a range of turbine to anchor speed ratio. It can be seen that, irrespective of the speed ratio, the co-rotating mode draws less power than the counter-rotating mode, and that the fixed anchor configuration is in fact also better (lower energy consumption for shorter mixing time discussed in the next section) than the counter-rotating mode. This quite surprising result goes the opposite way of industrial practice that favours the counter-rotating mode operation! Another interesting remark is the relatively low value of the transition regime threshold number at about  $Re = 15$ .

We show in Table 1 a comparison of the power consumption prediction with the measurements for the two rheological behaviours and two configurations considered for a speed ratio of 10. It can be seen that the predictions compare very well with the experiments for the Newtonian and non-Newtonian cases.

Table 2 gives the power constant values for the Maxblend impeller in the Newtonian case. Again, the agreement between the predictions and the experimental values is very good. These results show that the

Maxblend power draw is of the order of an anchor impeller, i.e. 60% of that of a double helical ribbon.

We show in Figure 4 the computed Maxblend power consumption in the Newtonian case. It can be seen that in the range of Reynolds number considered, there is no significant differences in terms of power consumption when baffling is used. Like with the coaxial mixer, the transition regime threshold number is relatively low at about  $Re = 70$ .

Operating conditions	$P_{Exp}$ (W)	$P_{Num}$ (W)
Co/Newt	82	81
Counter/Newt	113	108
Co/Non-Newt	3.5	3.7
Counter/Non-Newt.	6.5	6.1

**Table 1:** Coaxial mixer power consumption ( $N_a = 20$  RPM,  $N_r = 200$  RPM)

Baffles	$Kp_{Exp}$	$Kp_{Num}$
No	180	180
Yes	218	198

**Table 2:** Maxblend power constants

### Mixing Times

There are several ways of analysing mixing times results. We show for instance in Figure 5 the variation of the mixed volume vs. the number of revolutions for the

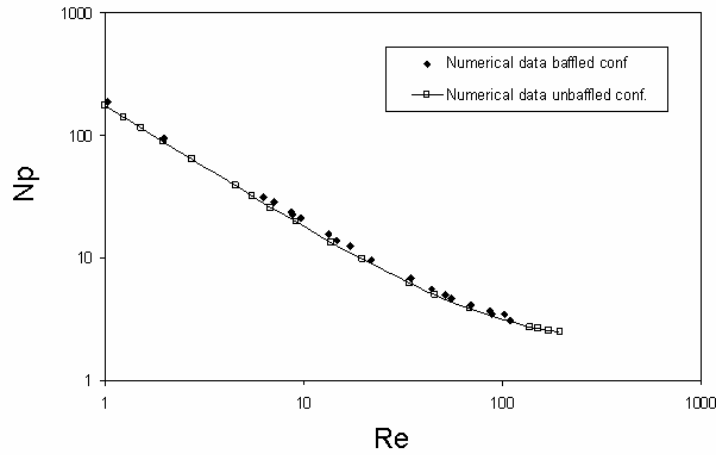


**Figure 4:** Maxblend power consumption (Newtonian case)

coaxial mixer. We defined here the mixed volume as the zone of intense agitation based on a percentage of the vessel volume where the flow speed is a preset fraction of the maximum tip speed (typically at least 5-10%).

It appears clearly that the mixed volume in the co-rotating mode is significant higher than with the counter-rotating mode at higher Reynolds number, as it covers almost the whole vessel volume. The situation degrades significantly at low Reynolds number, irrespective of the rotating mode. This is consistent with the fact that the anchor and the turbine rotate in the same direction allowing a synergetic action that has a strong positive influence on the mixing performance as already observed in previous investigations.

Figure 6 allows comparing the changes of the mixed volumes with respect to the fluid rheology. Not only, the mixed volume is shrunk in the counter-rotating mode, but this shrinking is enhanced with a non-Newtonian behaviour.

In this case, the mixed region occupies a reduced volume of fluid located immediately in the vicinity of the impeller. The fact that the Rushton turbine exhibits a radial discharge makes the extent of the region larger in the radial direction than in the axial one. This extreme situation is strongly linked with the presence of a cavern, called also working volume, around the impeller that the rotating anchor seems unable to destroy.

It is possible to explain these results by analyzing the flowfield in the vessel. As seen in Figure 7, the flow loops generated in the co-rotating mode are significantly larger than in the counter-rotating mode. However, the shearing action of the impeller is minimized in this mode making it less efficient for dispersion purposes. Therefore, a compromise must be found on the operating mode to use depending on the mixing task required.

Let us now turn our attention to the Maxblend impeller. This mixing problem will let us illustrate another piece of information useful in mixer design, which can be readily obtained by CFD, namely the intensity of segregation also called the coefficient of variation COV. We recall here that this parameter is defined as:

$$COV = \frac{\sqrt{\frac{\sum_{i=1}^{nel.} (c_i - c_{ave.})^2}{nel. - 1}}}{c_{ave.}}$$

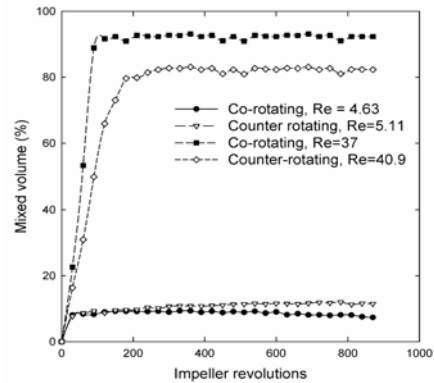


**Figure 5:** Numerical mixed volume vs. number of revolutions (coaxial mixer)

We show in Figure 8 the evolution of the intensity of segregation for 3 values of the Reynolds number in the non-baffled configuration. This result has been obtained by establishing a statistics of presence of the particles in the finite element cells.

Here again, the operation at higher Reynolds number closer to the transition regime yields significantly better results. The ideal value of zero segregation is not reached irrespective of the value of the Reynolds number considered, but there is an improvement by a factor of two between the intensity of segregation obtained in the strongly laminar case and that obtained at  $Re = 68$ .

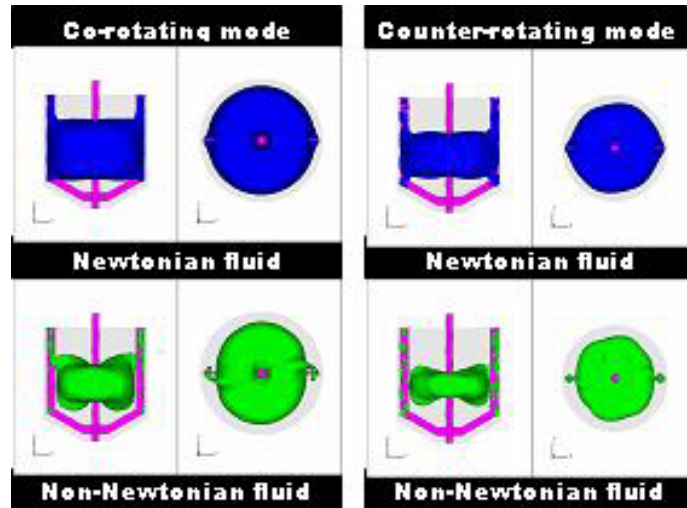


Figure 6: Effect of rheology on the mixed volume

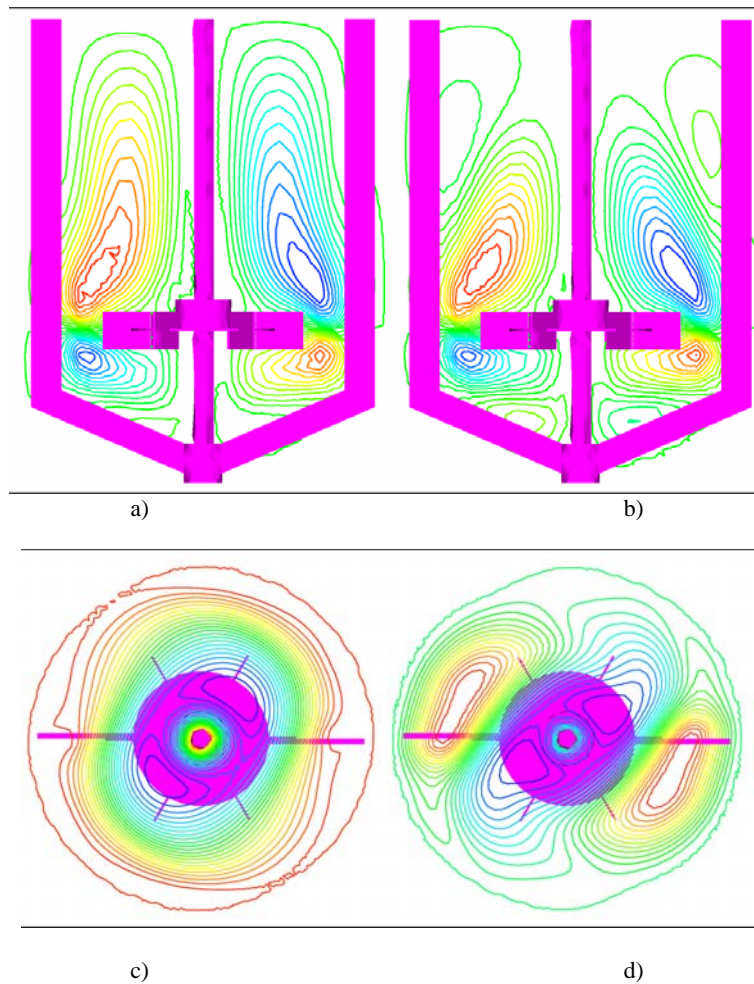
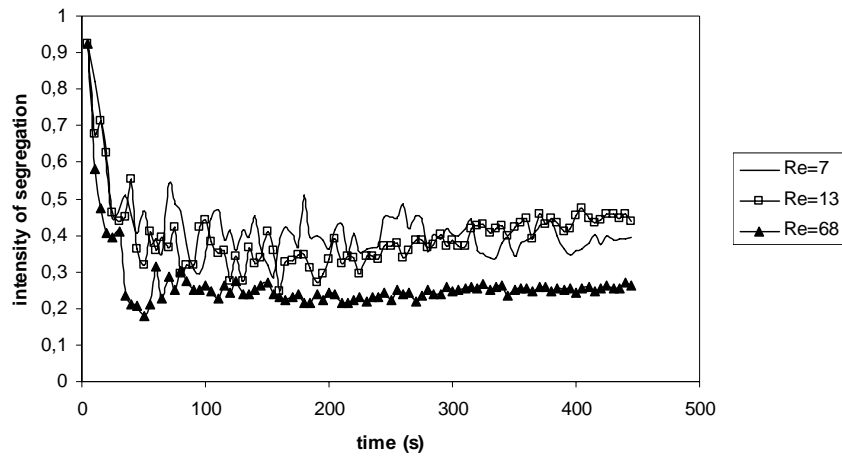


Figure 7: Streamlines for the coaxial system: (a): Co-rotation mode XZ plane (b): Counter-rotation mode XZ plane (c): Co-rotation mode XY plane (d): Counter-rotation mode XY plane



**Figure 8:** Evolution of the COV (Maxblend impeller)

The fluid mechanics in the Maxblend vessel seems to change drastically as the rotation speed is increased. Figure 9 gives a very clear picture on the flow phenomena generated by the Maxblend, in particular the secondary flow loops that are generated at low Reynolds number behind the paddle blades at the vessel bottom. These flow loops shrink when the rotation speed is increased and completely vanish in the transition regime. It must be noted that no secondary zones exist when the vessel is baffled as recommended by the manufacturer.

These secondary flow phenomena have consequences on the mixing time. We show in Figure 10 the variation of the mixing time with the Reynolds

number. Both experimental values and predictions are given. It is very clear that the baffled configuration outperforms the non-baffled configuration, even in the laminar regime, which is a pretty uncommon feature in mixing engineering. Also, the mixing times decrease when the Reynolds number is increased. This trend is logical as the power consumption is also larger.

Finally, considering the uncertainty existing in the experimental determination of the mixing time by the discoloration method, it can be seen that the agreement between the predictions and the experiments is very good.

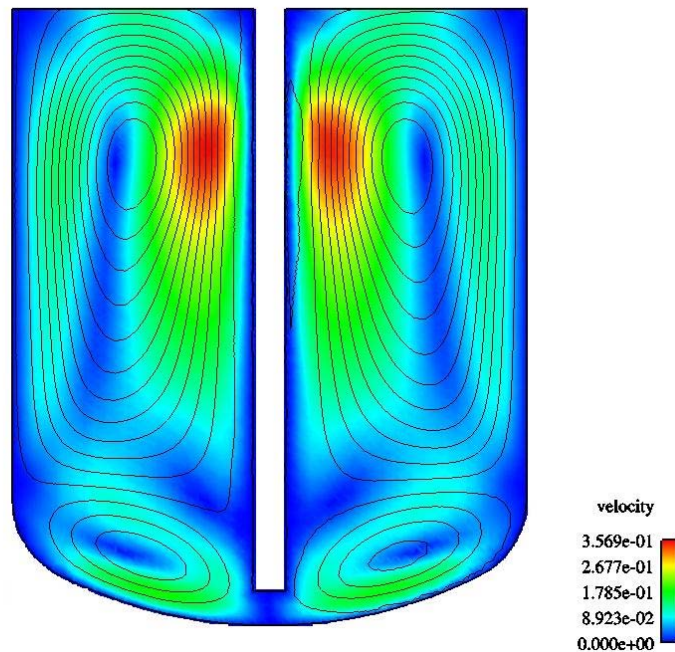


**Figure 9:** Velocity field in the Maxblend vessel (impeller plane)

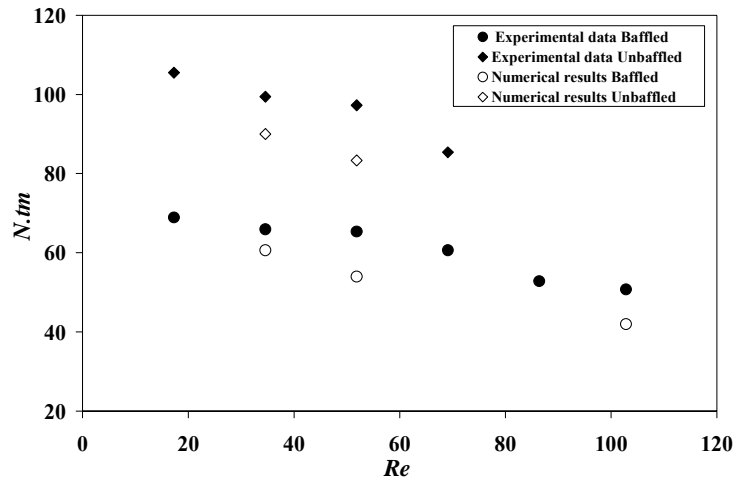


Figure 10: Effect of the baffles on mixing times

## CONCLUSION

The present study clearly demonstrates that the use of CFD for the study of “single phase” mixing with complex rheology and complex mixer configurations has now reached a level of maturity that makes it a practical tool to handle industrial mixer design problems. In this domain, like with other CFD applications, the focus is changing to the modelling of multiphase systems. The challenges in multiphase mixing simulations are enormous due to the complexity of the situations to be tackled. We can mention as an illustration the prediction of droplet size in emulsions, the dispersion of fillers in polymers at high loading rates, or the analysis of flotation at high solids which involves 3 phases and high slurry viscosities. Not only a good representation of the physics will be needed (closure models), but efficient algorithms will have to be developed to cope with the extreme non-linearities arising in those problems and the very large number of variables to consider.

## ACKNOWLEDGEMENTS

The technical and financial support of the members of Ecole Polytechnique’s Consortium on *Innovative Non-Newtonian Mixing Technologies* and NSERC is gratefully acknowledged.

## REFERENCES

BERTRAND, F., TANGUY, P.A., and THIBAUT, F. (1997), “A Three-Dimensional Fictitious Domain Method for Incompressible Fluid Flow Problems”, *Int. J. Num. Meth. Fluids*, **25**, 719-736.

FOUCAULT, S., ASCANIO, G., TANGUY, P.A. (2004), “Coaxial Mixer Hydrodynamics with Newtonian and non-Newtonian Fluids”, *Chem. Eng. and Technol.*, **27**, 324-329.

FREUND, R.W., (1993), “A transpose-free quasi-minimum residual algorithm for non-Hermitian linear systems”, *SIAM J. Sci. Comput.*, **14**, 470-482.

TAKAHASHI, K., HORIGUCHI, H., MISHIMA, M., YATOMI, R., (2006), “Mixing Characteristics in a vessel agitated by large paddle impeller Maxblend”, In: *Proceedings of 12<sup>th</sup> European Conference on Mixing*, Bologna, Italy.